Check for updates

View Article Online
View Journal

CrystEngComm

Accepted Manuscript

This article can be cited before page numbers have been issued, to do this please use: R. Dalapati, S. Balasubramanian, M. K. Ghosalya, D. Amarajothi and S. Biswas, *CrystEngComm*, 2017, DOI: 10.1039/C7CE01053B.

This is an Accepted Manuscript, which has been through the Royal Society of Chemistry peer review process and has been accepted for publication.

Accepted Manuscripts are published online shortly after acceptance, before technical editing, formatting and proof reading. Using this free service, authors can make their results available to the community, in citable form, before we publish the edited article. We will replace this Accepted Manuscript with the edited and formatted Advance Article as soon as it is available.

You can find more information about Accepted Manuscripts in the author guidelines.

Please note that technical editing may introduce minor changes to the text and/or graphics, which may alter content. The journal's standard Terms & Conditions and the ethical guidelines, outlined in our author and reviewer resource centre, still apply. In no event shall the Royal Society of Chemistry be held responsible for any errors or omissions in this Accepted Manuscript or any consequences arising from the use of any information it contains.

ROYAL SOCIETY OF CHEMISTRY

rsc.li/crystengcomm

Please do not adjust margins

View Article Online
DOI: 10.1039/C7CE01053B

Journal Name

ARTICLE

Published on 06 September 2017. Downloaded by Fudan University on 06/09/2017 04:30:45.

A cerium-based metal-organic framework having inherent oxidase-like activity applicable for colorimetric sensing of biothiols and aerobic oxidation of thiols

Received 00th January 20xx,
Accepted 00th January 20xx

DOI: 10.1039/x0xx00000x

www.rsc.org/

Rana Dalapati,[a] Balasubramanian Sakthivel,[b] Manoj K. Ghosalya,[c] Amarajothi Dhakshinamoorthy,*[b] and Shyam Biswas*[a]

A cerium-based metal-organic framework (MOF; **1**) with UiO-66 (UiO: University of Oslo) framework topology was synthesized solvothermally by employing 3,4-dimethylthieno[2,3-*b*]thiophene-2,5-dicarboxylic acid as a ligand. The MOF was thoroughly characterized by X-ray photoelectron spectroscopy (XPS), X-ray powder diffraction, infrared spectroscopy, themogravimetric and N_2 sorption analyses. The activated material (**1'**) retained its structural integrity in water, acetic acid and 1M HCl solution. XPS invetsigation reveals the presence of both Ce(III) and Ce(IV) ions in **1**. Owing to the presence of mixed-valence cerium ions, **1'** was able to oxidize the chromogenic peroxidase substrate 3,3′,5,5′-tetramethylbenzidine (TMB) or 2,2′-azinobis(3-ethylbenzothizoline-6-sulfonic acid) (AzBTS) in the absence of an external oxidizing agent. Thus, it showed inherent oxidase-like catalytic properties. Inspired by the excellent oxidase-mimic activity of **1'**, a protocol was developed for the rapid colorimetric sensing of biothiols in NaAc buffer (0.2 M, pH = 4). The sensing ability of **1'** towards cysteine was also demonstrated in human blood plasma. Furthermore, the redox-active cerium ions enabled **1'** to exhibit excellent heterogeneous catalytic performance in aerobic oxidation catalysis of thiol compounds. The material is reusable (both as sensor and catalyst), low-cost and highly stable, which renders it a promising candidate for monitoring of biothiols in immunoassays and medical diagnosis as well as for industrial oxidation catalysis.

Introduction

Colorimetric sensing technique has gained immense attention in biology and analytical chemistry owing to its easy visual readout and rapid visual determination with naked eyes or low-cost portable instruments.[1] Colorimetric biosensors are capable of showing response towards target biomolecules (cysteine, glutathione, homocysteine, thiamine, glucose, ascorbic acid, etc.) through a change in colour.[2] Detection of these species is highly desirable, since they play vital roles in different physiological processes such as metabolism, protein synthesis, detoxification and reversible redox reaction.[3] For the sensing of biomolecules, optical,[4] electrochemical[5] and bio-electrochemical[6] sensing techniques are extensively employed. However, these methods have considerable disadvantages like absence of rapidity, selectivity and sensitivity. Moreover, the bio-enzymes easily undergo denaturation or chemical changes upon heating. In addition, the preparation, storage and purification of enzymes require too much time.[7,8] Hence, numerous analogous materials such as Fe_3O_4,[9] Au nanoparticles,[10] graphene oxide[11] and carbon dots[12] have been investigated. Since the catalytic performances of these materials are analogous to those of natural enzymes, their enzyme-mimic characteristics have been utilized for the sensing of biological analytes. The major advantages of these analogous materials include facile and controlled synthesis having high yield, lower cost, adjustable catalytic performances, and tunable structure and composition.[13] Because of these benefits, enzyme-mimetic nanomaterials have attracted widespread attention. These materials exhibit similar catalytic activity as natural oxidases or peroxidases and hence they have been efficiently utilized as biosensors for applications in environmental monitoring and biomedical diagnosis.[2]

The oxidation of thiols to disulfides has drawn immense interest since the disulfides play vital roles in many biochemical and industrial processes.[14] In the industry, disulfides are used in synthesis of pharmaceuticals, agrochemicals and vulcanization of rubber.[15] Furthermore, the

[a] *Department of Chemistry, Indian Institute of Technology Guwahati, 781039 Assam, India. E-mail: sbiswas@iitg.ernet.in; Fax: +91 3612582349; Tel: +91 3612583309*
[b] *School of Chemistry, Madurai Kamaraj University, 625021 Madurai, Tamil Nadu, India. E-mail: admguru@gmail.com*
[c] *Catalysis Division, National Chemical Laboratory, Dr. Homi Bhabha Road, Pune 411008, India.*

†Electronic Supplementary Information (ESI) available: XPS and IR spectra, TG-curves, XRPD patterns, FE-SEM images, absorption spectra and GC traces. See DOI: 10.1039/x0xx00000x

CrystEngComm Accepted Manuscript

Please do not adjust margins

View Article Online
DOI: 10.1039/C7CE01053B

Published on 06 September 2017. Downloaded by Fudan University on 06/09/2017 04:30:45.

protection of thiols can be easily achieved through the formation of disulfides and conversely the cleavage of disulfide bonds leads to the formation of thiols.[16] The oxidation of thiol compounds is an effective method for the industrial production of disulfides because of the commercial availability of many thiols and their convenient preparation procedures. However, many over-oxygenated by-products such as sulfoxides and sulfones can be produced during the oxidation of thiols. On the other side, the selective oxidation of thiols to disulfides have been so far accomplished through the employment of a variety of reagents such as Ce(IV) salts, permanganates, peroxides, air along with transition-metal oxides, sodium chlorite, sodium perborate, halogens, nitric oxide and ferric chloride.[17]

Metal-organic frameworks (MOFs) have received tremendous attention in last two decades since they have shown application potentials in chemical sensing, gas adsorption and separation, heterogeneous catalysis and drug delivery.[18-20] Until today, few Fe(III)-containing MOFs such as MIL-53, MIL-88A, MIL-68, MIL-100, MIL-88-NH_2 and MIL-101 have been reported, which have exhibited inherent peroxidase-like catalytic behaviour applicable for colorimetric biosensing.[21-28] These examples also include two Zr(IV)-based MOFs having Fe(III)-metalated porphyrin ligands.[29-31] However, only two M(IV)-based (M = Zr, Ce) single-metal MOFs have been employed so far to demonstrate the oxidase-like activity for biosensing. These MOFs include a mixed-valence (Ce^{3+}/Ce^{4+}) Ce-MOF (called MVCM)[32] and Zr(IV)-based MOF UiO-66-NH_2[33]. Among various MOFs that have displayed either oxidase- or peroxidase-like activity, facile colorimetric sensing for biothiols have been demonstrated only for Fe-MIL-88-NH_2,[31] MVCM and Zr-UiO-66-NH_2. On the other hand, only two MOFs namely Fe(BTC) and Fe-MIL-100 have been demonstrated to accomplish oxidation catalysis of thiols to disulphides using molecular oxygen.[18, 34]

Cerium oxide nanoparticles (nanoceria) occurs as mixed valence state oxides of Ce^{3+} and Ce^{4+}, and are able to reversibly switch between the two oxidation states.[35] Due to this phenomenon, nanoceria has featured oxidase-mimic characteristics beneficial for colorimetric biosensing.[36-38] Furthermore, the MVCM material has been recently reported to sense biothiols colorimetrically due to its oxidase-mimic features.[32] On the other hand, few Ce(IV) complexes have been employed to accomplish oxidation of thiol compounds to disulphides in the homogeneous phase using molecular oxygen.[39] In addition, the ability of cerium(IV) ammonium nitrate (CAN) to act as a homogeneous oxidation catalyst has been demonstrated in various substrates including alcohols, thioethers, epoxides, alkylbenzenes and active methylene compounds.[40] However, until now, there is no report on Ce-based MOFs showing catalytic activity for colorimetric biosensing of thiols as well as aerobic oxidation of thiols. Encouraged by the richness of cerium chemistry in colorimetric sensing and oxidation catalysis, we have synthesized a Ce-based MOF (**1**) incorporating 3,4-dimethylthieno[2,3-*b*]thiophene-2,5-dicarboxylic acid (H_2DMTDC) as ligand. The presence of both Ce(III) and Ce(IV) ions in the framework was confirmed by XPS analysis. The activated MOF (**1'**) features an inherent oxidase-mimic behaviour in NaAc buffer at acidic pH, since it is capable of performing rapid oxidation of chromogenic peroxidase substrates like 3,3',5,5'-tetramethylbenzidine (TMB) or 2,2'-azinobis(3-ethylbenzothizoline-6-sulfonic acid) (AzBTS) without the need of any external oxidizing agent (e.g. H_2O_2). On the basis of these outcomes, we have established a colorimetric sensing platform for biothiols in NaAc buffer (pH = 4.0) as well as in human blood plasma. Moreover, the heterogeneous catalytic activity of **1'** for oxidation catalysis of thiol compounds to disulphides using molecular oxygen has been thoroughly investigated.

Experimental

Materials and synthetic procedures

The synthesis of H_2DMTDC ligand was accomplished by following a formerly documented protocol.[41] All the other reagents were procured from commercial vendors. The infrared (IR) spectra in the range 440-4000 cm^{-1} were collected with a Perkin Elmer Spectrum Two spectrometer. To describe absorption bands, the following notations were used: broad (br), shoulder (sh), weak (w), strong (s), medium (m) and very strong (vs). Thermogravimetric analyses (TGA) were carried out by a Mettler-Toledo TGA/SDTA 851e thermogravimetric instrument in a temperature range 25-700 °C with a heating rate of 5°C min^{-1} in air atmosphere. X-Ray powder diffraction (XRPD) measurement were performed with a Bruker D2 Phaser X-ray diffractometer (10 mA, 30 kV) utilizing Cu-*K*α (*λ* = 1.5406 Å) radiation. X-ray photoelectron spectroscopy (XPS) measurement was carried out at room temperature using a custom-built near-ambient pressure photoelectron spectrometer (Prevac, Poland) and full details are available in ref. 18 and 19. It is equipped with R3000HP analyser (Scienta) with a twin-anode and monochromatic (Al-*K*α) X-ray source. However, the experiment was carried out with Mg-*K*α (hν = 1253.6 eV) source. The base pressure in the analysis chamber was kept in the 3 to 6 × 10^{-10} mbar range. The energy resolution of the spectrometer was set at 0.7 eV with Mg-*K*α radiation at a pass energy of 20 eV. The calibration for the binding energy (BE) was carried out with the Au($4f_{7/2}$) core level at 84.0 eV. Field emission - scanning electron microscopy (FE-SEM) images were collected by Zeiss (Zemini) scanning electron microscope. UV-vis spectra in the region 250-800 nm were recorded with a Perkin Elmer Lambda 25 UV-vis spectrometer. All solutions for the UV-vis measurements were prepared by using Milli-Q water. The nitrogen adsorption experiments at -196 °C were carried out employing a Quantachrome Autosorb iQ-MP volumetric gas adsorption equipment. Before the adsorption measurement, the degassing of the sample was accomplished by heating at 70°C for overnight in high vacuum. Conversion and selectivity were determined using Agilent 7820 gas chromatography with FID. To identify the products, gas chromatography – mass

CrystEngComm Accepted Manuscript

This journal is © The Royal Society of Chemistry 20xx

Please do not adjust margins
View Article Online
DOI: 10.1039/C7CE01053B

Published on 06 September 2017. Downloaded by Fudan University on 06/09/2017 04:30:45.

spectrometry (GC-MS) measurements were performed with Perkin Elmer Clarius 500 spectrometer.

Synthesis of $[Ce_6O_4(OH)_4(DMTDC)_6].2DMF.22H_2O$ (1)

A mixture of H_2DMTDC (40 mg, 0.16 mmol) in 2 mL of *N,N*-dimethylformamide (DMF) was sonicated until it dissolved completely. Consequently, ceric ammonium nitrate (CAN) was added as an aqueous solution (400 µL, 0.533 M). The mixture was put inside a glass tube, which was sealed. This tube was heated at 100 °C for 3.5 h by means of a dry block heater. The mixture was cooled down to ambient temperature and the light yellow precipitate was filtered off. This precipitate was washed twice with DMF and once with acetone. The resulting solid was dried in an oven at 70 °C for 6 h and denoted as **1**. Yield of the compound was 48 mg (0.02 mmol, 46%) considering the Ce salt. Anal. calcd for $C_{66}H_{98}Ce_6N_2O_{56}S_{12}$ (3040.95 g mol^{-1}): C, 26.06 H, 3.24 N, 0.921. Found: C, 26.74 H, 3.18 N, 1.02%. FT-IR (KBr, cm^{-1}): 3430 (br), 2927 (w), 2852 (w), 1647 (s), 1605 (sh), 1495 (m), 1378 (vs), 1268 (w), 1158 (sh), 1103 (m), 1019 (w), 799 (sh), 772 (m), 662 (w), 558 (m), 469 (w).

Activation of as-synthesized 1

At first, the as-synthesized material (0.2 g) was stirred in methanol (20 mL) for 24 h at ambient temperature. Then, the yellow material was filtered off. The degassing of the solid was accomplished by heating at 70 °C for 16 h in high vacuum. In this way, the activated material (denoted as **1'**) was obtained.

Oxidase-like activity of 1'

For performing the UV-vis experiments, aqueous suspensions of **1'** (concentration: 1 mg/mL) were made by ultrasonic treatment for 30 min. For examining the oxidase-like activity, the catalytic oxidation of 3,3',5,5'-tetramethylbenzidine (TMB) was investigated to obtain a blue coloured solution. For this purpose, 120 µL aqueous suspension of **1'** and 100 µL of TMB solution (0.04 mM) were added to 2780 µL of NaAc buffer (0.2 M, pH = 4.0). The influence of reaction time on absorbance (λ_{max} = 652 nm) of ox-TMB was examined by measuring UV-vis spectra of the resulting mixture at a regular time interval (2 min) until the absorbance of ox-TMB became saturated. For investigation of the steady-state reaction mechanism, additional UV-vis measurements were carried out under similar conditions as mentioned above, except that various concentrations of TMB solution were added to the suspension.

Detection of biothiols in NaAc buffer

The colorimetric method for the detection of biothiols involve the following steps: initially, 2680 µL of 0.2 M NaAc buffer (pH = 4.0), 120 µL of TMB solution (1 mM, ethanol solution) and 100 µL aqueous suspension of **1'** (1.0 mg mL^{-1}) were mixed together to get a blue coloured solution of ox-TMB. After the absorbance of ox-TMB was saturated, 100 µL of a biothiol solution (0.5 mM) was added and the UV-vis spectrum of the resulting mixture was recorded. Analogous experiments were also carried out by replacing the biothiols with the following possibly interfering biomolecules: aspartic acid, alanine, arginine, proline, glycine, isoleucine, lysine, histidine, leucine, phenylalanine, threonine, methionine, valine, tryptophan and serine. In order to determine the selectivity of **1'** towards biothiols co-existing with other biomolecules, the above-mentioned procedure was followed, except the sequential addition of two amino acid solutions (i.e. interfering biomolecules followed by biothiols) in the last step instead of one amino acid (i.e. biothiols) solution.

Detection of biothiols in human blood plasma

From the left arm vain, 5 mL of human blood was collected in a tube having ethylenediaaminetetraacetic acid (EDTA) under aseptic conditions. For the separation of plasma, the blood was centrifuged at 3000 rpm for 5 min. Afterwards, the straw-coloured supernatant human blood plasma (HBP) was collected and employed for the further experiments. 160 µL of HBP was placed in four microcentrifuge tubes and different amounts of cysteine solutions were spiked. After that, incubation of the mixture was accomplished at 37 °C for 5 min. Later, 200 µL of 60% (v/v) acetonitrile was added to this mixture for precipitating the proteins. Then, the mixture was centrifuged at 6000 rpm for 5 min for the complete separation of the proteins. The resulting supernatant solution was used further for sensing cysteine in a similar method as the sensing of cysteine in NaAc buffer. A control experiment was also carried out without spiking the cysteine.

Aerobic oxidation catalysis

A typical reaction was performed in which thiophenol (1 mmol) and 2 mL of methanol were poured in a 25 mL round-bottom flask and catalyst **1'** (20 mg) was added to it. The reaction mixture was stirred at 70 °C in a preheated oil bath and oxygen from a balloon was purged into it. The progress of the reaction was regulated by GC through sampling aliquots at various time gaps. Heterogeneity of the catalytic reaction was performed as indicated above, except that the catalyst was filtered after 2 h from the reaction mixture using a 0.2 µm PTFE filter and then the reaction was continued up to 12 h in the absence of the catalyst. In addition, the stability of the catalyst was checked by performing reusability experiments under the optimized reactions conditions. After the reaction, **1'** was filtered, washed twice with methanol and then washed thoroughly with acetone for the exclusion of all unreacted compounds from the catalyst. Afterwards, the material was dried at 80 °C for 16 h in a traditional oven. This dried compound (**1'**) was used as the catalyst in the subsequent catalytic runs.

CrystEngComm Accepted Manuscript

Please do not adjust margins

View Article Online
DOI: 10.1039/C7CE01053B

Published on 06 September 2017. Downloaded by Fudan University on 06/09/2017 04:30:45.

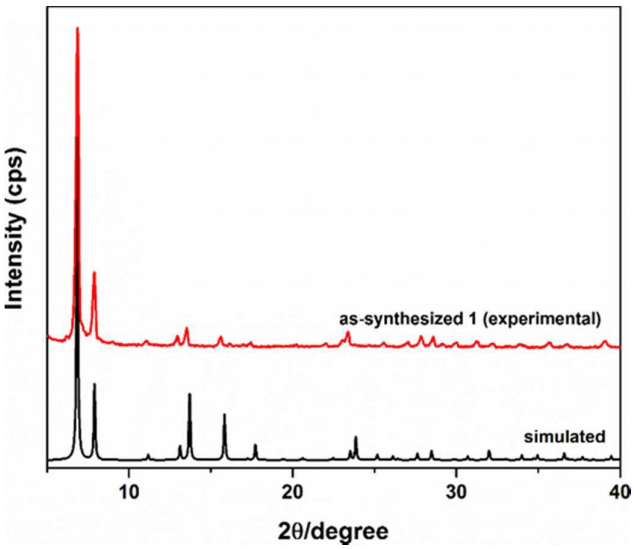

Fig. 1 Simulated (black) and experimental (red) XRPD patterns of **1**.

Results and discussion

Preparation and activation procedure

Compound **1** was synthesized by heating a mixture of aqueous ammonium cerium(IV) nitrate and 3,4-dimethylthieno[2,3-*b*]thiophene-2,5-dicarboxylic acid (H_2DMTDC) ligand in *N,N*-dimethylformamide (DMF) at 100 °C for 3.5 h. In order to remove the occluded DMF molecules, the as-synthesized material was first stirred in methanol. Later, the methanol molecules were removed from the cages by heating the methanol-exchanged material in high vacuum at 80 °C for 12 h. In this way, the activated material (termed as **1'**) was obtained.

Structure description

The experimental XRPD pattern of the as-synthesized form of **1** matches closely with the theoretical XRPD pattern of its previously reported, Zr(IV) analogue having UiO-66 type of framework topology (Fig. 1).[42, 43] Therefore, both **1** and its Zr(IV) analogue have the same framework topology as that of UiO-66.[44] The XRPD pattern of the as-synthesized compound can be successfully indexed in a cubic crystal system. The unit cell parameters of **1** (Table S1, ESI†) are very similar with the isostructural Zr(IV)-containing material.[42, 43] The framework structure of the isostructural Zr(IV) material has been described formerly by us.[42, 43] Briefly, the cubic framework structure (Fig. 2) of the title compound comprises hexanuclear cluster cores[45] having composition $[Ce_6O_4(OH)_4]^{12+}$. In these cluster cores, the six cerium atoms are situated at the corners of an octahedron. The eight faces of each octahedron are bridged by the O atoms of μ_3-O and μ_3-OH groups, which are arranged in an alternative fashion. Eight O atoms are coordinated with each Ce atom. The latter has square-antiprismatic geometry in which the O atoms from the carboxylate, μ_3-O and μ_3-OH groups occupy the square faces. Each $[Ce_6O_4(OH)_4]^{12+}$ cluster core is linked with the carboxylate groups of twelve DMTDC ligands. The chemical structure of the H_2DMTDC ligand is shown in Fig. 2e. The cubic, 3D framework of **1** is formed by the interconnection of the cluster cores by the carboxylate groups of adjacent ditopic DMTDC ligands. The structure incorporates two types of cages: larger octahedral and smaller tetrahedral. Eight tetrahedral cages surround each central octahedral cage. Both cage types are accessible to guest molecules via narrow triangular windows. The methyl groups attached with the DMTDC ligands are located at the triangular windows. These methyl groups project towards the inner side of the octahedral cages.

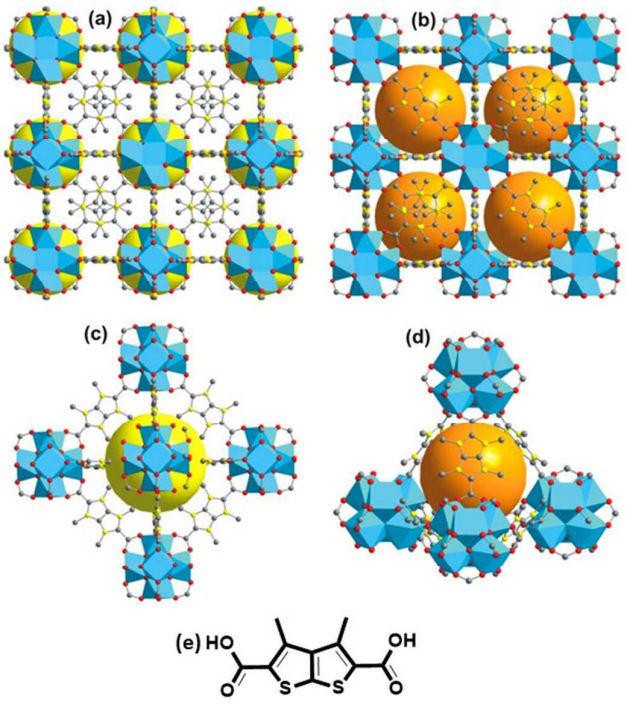

Fig. 2 Cubic 3D framework structure of **1** in ball-and-stick representation. (a, b) Depiction of octahedral (yellow spheres) and tetrahedral (orange spheres) cages. (c, d) are the magnified views of (a, b), respectively. (e) Structure of the H_2DMTDC ligand. Colour codes: Ce, blue polyhedra; C, grey; O, red; S, yellow.

Material characterization

The oxidation state of cerium in **1** was investigated by XPS analysis. The XPS study reveals that both Ce(III) and Ce(IV) ions are present in the framework of **1** (Fig. S1, ESI†).[46] The Ce 3d core level spectrum was analyzed to explore the oxidation state of Ce. The deconvolution of the Ce 3d core level spectrum suggests the presence of ten peaks. The six peaks at 883.1, 888.5, 898.4, 902.1, 907.5 and 916.8 eV correspond to the Ce(IV) state, whereas the Ce(III) state gives rise to four peaks at 880.6, 885.6, 900.0 and 904.8 eV.[46-48] The relative amount of Ce(III) ion present in **1** was determined to be 23.6% by utilizing the peak area of the deconvoluted core level spectrum.[49] The reducing ability of the DMF solvent with

CrystEngComm Accepted Manuscript

This journal is © The Royal Society of Chemistry 20xx

Please do not adjust margins
View Article Online
DOI: 10.1039/C7CE01053B

Published on 06 September 2017. Downloaded by Fudan University on 06/09/2017 04:30:45.

prolonged reaction time at high temperature might be responsible for the reduction of the Ce(IV) ions.[50]

In the IR spectra (Fig. S2, ESI†) of as-synthesized and activated **1**, absorption peaks with high intensity are observed at around 1595 and 1385 cm^{-1}. These peaks occur due to the asymmetric and symmetric $–CO_2$ stretching vibrations of the framework DMTDC ligands, respectively.[51, 52] The IR spectrum of as-synthesized **1** contains medium absorption peak at around 1650 cm^{-1}, which is attributable to the stretching vibrations for the carbonyl group of DMF molecules residing inside the pores. The IR spectrum of the activated compound does not contain any absorption peak for the occluded DMF molecules. The results from the FT-IR analysis confirm the complete activation of the compound.

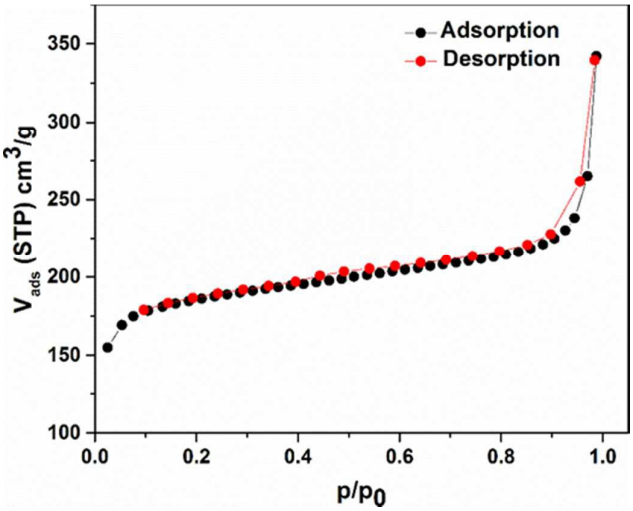

Fig. 3 N_2 sorption isotherms of **1'** collected at -196 °C.

In order to check the permanent porosity of activated **1'**, N_2 sorption experiments were conducted. In Fig. 3, the N_2 sorption isotherms of **1'** are displayed. The N_2 sorption isotherms follow a type-I behaviour according to the IUPAC classification. From the N_2 adsorption isotherm, the specific BET surface area and micropore volume (at p/p_0 = 0.5) of **1'** were calculated to be 1020 m^2 g^{-1} and 0.65 cm^3 g^{-1}, respectively.

To investigate the thermal stability of **1** and **1'**, thermogravimetric analyses were performed in the range 25-700 °C under air atmosphere. From the TG traces (Fig. S3, ESI†), it can be concluded that the material is stable up to 300 °C. The first weight loss of 13.2 wt% (range: 40-150 °C) in the TG trace of as-synthesized **1** occurs because of the removal of 22 guest H_2O molecules per formula unit (calcd.: 13.0 wt%). In the range 150-210 °C, the second weight loss of 5.0 wt% takes place due to the removal of 2 occluded DMF molecules per formula unit (calcd.: 4.86 wt%). After 210 °C, the material starts to decompose on account of the loss of framework ligands.

The TG trace of activated **1'** contains one weight loss stage below the decomposition temperature which is observed because of the removal of the adsorbed water molecules from the pores. The activated material adsorbs water (moisture) from air during storage under ambient conditions before the TG measurement.

For checking the chemical stability of activated **1'**, the samples (0.1 g) were stirred in various liquids such as water, 1M HCl and acetic acid (15 mL for each liquid) at ambient temperature for 12 h. Then, the samples were filtered off and XRPD experiments were carried out for checking their crystallinity. Fortunately, the crystallinity of the compound was did not change upon stirring in these liquids, which became obvious from their XRPD patterns (Fig. S4, ESI†). The high stability of the material in both aqueous and acidic medium encouraged us to investigate its oxidase-like catalytic activity in acidic medium.

To check the phase-purity and morphology of **1'**, FE-SEM images were collected. The FE-SEM images (Fig. S5, ESI†) confirm the homogeneous crystalline nature of **1'** (consisting of octahedral particles) and the absence of any impure phase.

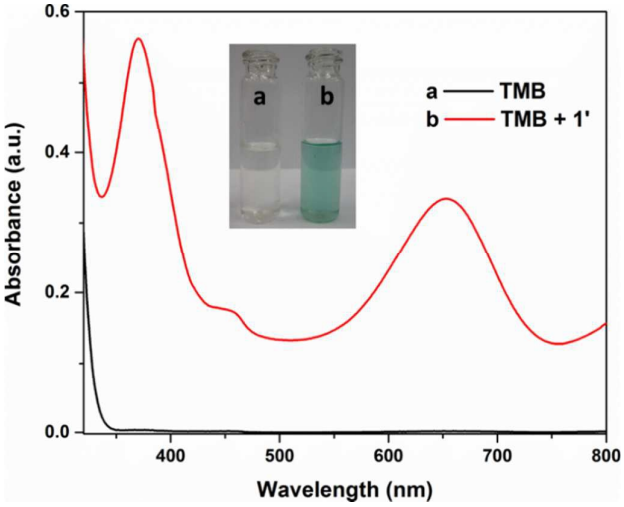

Fig. 4 UV-vis spectra of 0.04 mM TMB (a) with and (b) without **1'** (13.3 μM) in NaAc buffer (0.2 M, pH = 4) at room temperature. Inset: corresponding chromogenic change of TMB.

Oxidase-mimic properties

At first, we have explored the ability of **1'** to oxidize peroxidase substrates in acidic medium. For this purpose, we have chosen two typical chromogenic peroxidase substrates, namely 2,2-azinobis (3-ethylbenzothizoline-6-sulfonic acid) (AzBTS) and 3,3',5,5'-tetramethylbenzidine (TMB). Either a blue (for ox-TMB) or green (for ox-AzBTS) color is produced when these substrates are oxidized in aqueous medium. These substrates have been previously employed for examining the peroxidase-like activity of several MOF materials[23, 24, 26, 28, 53-67] where H_2O_2 is employed as an oxidizing agent. On the other hand, the present cerium-based **1'** is capable of oxidizing both AzBTS and

CrystEngComm Accepted Manuscript

Please do not adjust margins

View Article Online
DOI: 10.1039/C7CE01053B

Published on 06 September 2017. Downloaded by Fudan University on 06/09/2017 04:30:45.

TMB without any external oxidizing agent such as H_2O_2. These facts have been verified by the visual color changes of the dye molecules in NaAc buffer (pH = 4) in presence of **1'** and the corresponding drastic changes in the UV-vis spectra. The pH-dependent investigation disclosed that the optimal pH value for the oxidase-like activity of **1'** is ca. 4. The pH values higher or lower than 4 led to decrease in the oxidase-mimic activity of the MOF towards TMB (Fig. S6, ESI†). For TMB, the formation of a blue colored solution having absorption maxima at 652 and 370 nm (Fig. 4) confirms the formation of the oxidized product (denoted as ox-TMB).[68] In case of AzBTS, the new absorption bands appeared at around 415 and 644 nm, which corroborates the generation of $ABTS^{\cdot+}$ radical (Fig. S7, ESI†).[69] The green color was developed within one minute, which indicates a rapid oxidation of the dye molecule by **1'**. We have systematically studied the influence of catalyst amount on the catalytic activity of **1'**. The change in the absorbance (monitored at 652 nm) of TMB as a function of time upon addition of various amounts of **1'** is plotted in Fig. 5. This figure reveals that the catalytic activity of **1'** increases when increasing amounts of its suspension are added to the reaction medium. Furthermore, the recyclability of **1'** towards the catalytic oxidation of TMB was investigated up to 4 cycles. The results confirmed that the MOF material is highly stable and reusable up to 4 cycles under the optimized reaction conditions (Fig. S8-S9, ESI†).

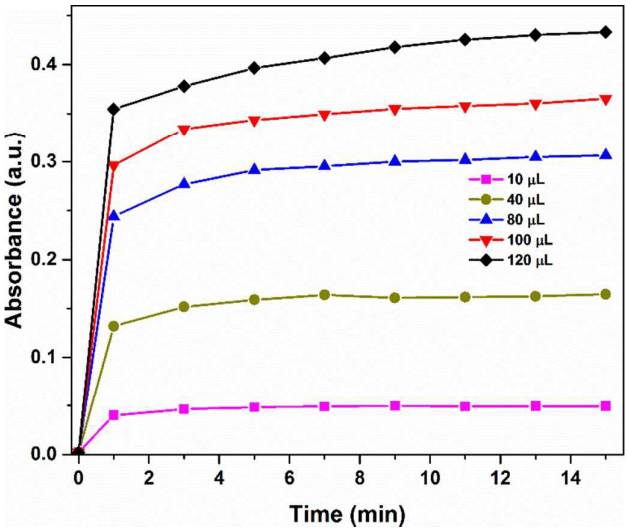

Fig. 5 Time-dependent variation in the absorbance of TMB (monitored at 652 nm) upon addition of various amounts of **1'** in NaAc buffer (0.2 M, pH = 4).

Since **1'** displayed oxidase-like activity, the apparent steady-state kinetic parameters were evaluated for the oxidation of TMB by **1'**. For this purpose, the concentration of TMB was varied. To analyze the kinetic parameters, a typical Michaelis-Menten equation was employed. Lineweaver–Burk plot (Fig. S10, ESI†) was used in order to evaluate the maximum initial velocity (V_{max}) and Michaelis-Menten constant (K_m). From this plot, the values of K_m and V_{max} were estimated to be 88 µM and 0.11 µM s^{-1}, respectively. The K_m value for **1'** is lower than natural enzyme called horseradish peroxidase (HRP),[50] recently reported Ce-MOF called MVCM[32] as well as nanoceria[36] (Table S2, ESI†). This K_m value suggests that the affinity of **1'** towards TMB molecule is higher as compared to HRP, MVCM as well as nanoceria.

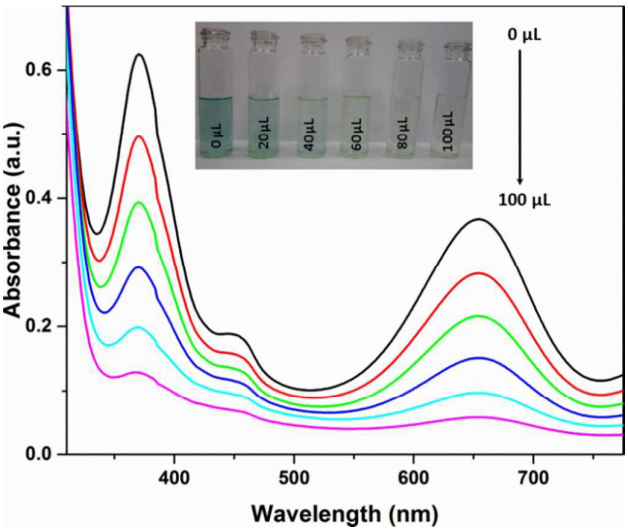

Fig. 6 Change in the absorption spectrum of ox-TMB upon gradual addition of 0.5 mM cysteine solution in NaAc buffer (0.2 M, pH = 4). Inset: corresponding change in color of the ox-TMB solution.

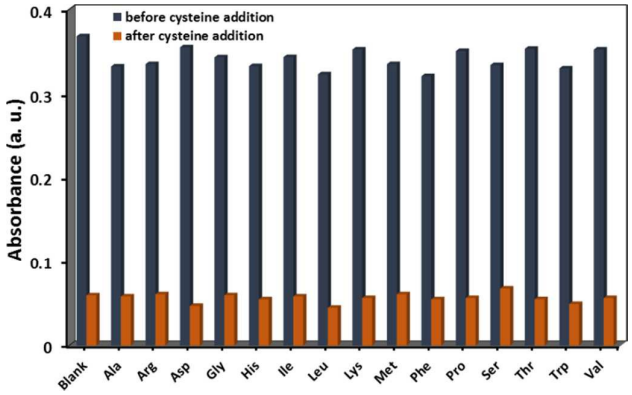

Fig. 7 Absorbance of ox-TMB (monitored at 652 nm) upon addition of a potentially competing amino acid, followed by the addition of cysteine in NaAc buffer (0.2 M, pH = 4).

The mechanism of the oxidase-like activity of Cerium-based **1'** towards TMB may be related to the $Ce^{4+} \leftrightarrow Ce^{3+}$ spontaneous electron shuttling through the framework system.[32] When TMB solution was added to the suspension of **1'** in NaAc buffer (0.2 M, pH = 4.0), the Ce^{4+} ions quickly oxidize TMB to form blue-coloured ox-TMB. During this process, Ce^{4+} ions are reduced to Ce^{3+} ions. Then, the latter is naturally converted to the Ce^{4+} ions.

CrystEngComm Accepted Manuscript

This journal is © The Royal Society of Chemistry 20xx

Please do not adjust margins
View Article Online
DOI: 10.1039/C7CE01053B

Published on 06 September 2017. Downloaded by Fudan University on 06/09/2017 04:30:45.

Detection of biothiols in NaAc buffer

It has been previously reported that biological thiols (biothiols) have the capability to reduce the blue-coloured ox-TMB in aqueous medium, leading to the formation of colourless TMB.[31, 32, 70, 71] Encouraged by this fact, we have developed a colorimetric protocol for the sensing of biothiols. The UV-vis spectra of ox-TMB comprising **1'** in NaAc buffer (0.2 M, pH = 4) were recorded with incremental addition of 0.5 mM solutions of various amino acids (including alanine, cysteine, aspartic acid, arginine, histidine, glycine, leucine, isoleucine, lysine, phenylalanine, methionine, serine, proline, tryptophan threonine and valine) and other thiol-containing biomolecules (such as homocysteine and glutathione). Among the different amino acids and thiol-containing biomolecules added, a rapid decolourization of ox-TMB was observed upon addition of biothiol compounds such as glutathione, cysteine and homocysteine. It can be seen from Fig. 6 and Fig. S11-S13 (ESI†) that the absorbance of ox-TMB decreased dramatically upon gradual addition of 0.5 mM solutions of cysteine, homocysteine and glutathione. In sharp contrast, negligible change in the absorbance of ox-TMB was observed in the presence of other possibly interfering biomolecules (Fig. S14-S28, ESI†). Even methionine, another sulphur-containing amino acid, resulted in negligible change in the absorbance of ox-TMB under the presented conditions. These phenomena can be understood considering that after oxidation of TMB by the MOF catalyst to produce bluish coloured ox-TMB, the biothiols reverses the process by reduction of ox-TMB back to colourless TMB. The results presented herein suggest that **1'** shows high selectivity towards the sensing of biothiols (glutathione, cysteine and homocysteine).

In order to investigate the selectivity of **1'** towards the sensing of biothiols, the UV-Vis spectral response of the MOF system (i.e., **1'** containing ox-TMB in aqueous medium) was measured towards biothiols in the existence of several potentially interfering amino acids. It has been observed that the absorbance of the MOF system changed significantly only after the introduction of biothiols to the reaction medium, whereas the introduction of other amino acids caused negligible changes in the absorbance (Fig. 7 and Fig. S29-S43, ESI†). Therefore, the selective colorimetric sensing of biothiols in presence of other potentially competing amino acids can be achieved by this method.

For determining the limit of detection (LOD) of **1'** towards biothiols, very less concentrated biothiol solutions were slowly added to the reaction medium and the absorbance of ox-TMB was monitored. The plots of absorbance of ox-TMB against the concentration of biothiol solutions revealed linear curves (Fig. S44-S46, ESI†). The LOD values were estimated from this linear curve by following the previously reported method.[50] The LOD values for cysteine, homocysteine and glutathione by this colorimetric biosensing technique were estimated to be 0.150, 0.132 and 0.125 μM, respectively. These LOD values are either similar or lower as compared to the previously reported MOFs (Table S3, ESI†)[31, 33, 72] exhibiting selective detection properties towards biothiols.

Detection of biothiols in human blood plasma

It is well known that human blood plasma contains high concentrations of cysteine (165-335 μm),[73] homocysteine (9-13 μM)[74] and glutathione (14-20 μm).[75] Therefore, the ability of **1'** to detect cysteine in human blood plasma (HBP) was evaluated. The concentration of cysteine in HBP samples was determined by utilizing the standard addition method. The recovery experiments were carried out with two HBP samples spiked with cysteine. As shown in Table 1, the recovery for cysteine measurement ranges from 98 to 102% with low RSD (n = 3) values. These results verify the suitability of the developed protocol for the sensing of cysteine in HBP samples.

Table 1. Concentrations of cysteine found in diluted HBP samples determined by the standard addition technique.

HBP Sample	Without Spiking (μM)	Cysteine Added (μM)	Cysteine Found (μM)	Recovery (%)	RSD (%)
Sample 1	65.4	10	9.8	98	1.8
		50	50.1	100.2	2.1
Sample 2	110.5	10	0.1	101	1.6
		50	51.2	102.4	1.2

Catalytic oxidation of thiol compounds

MOFs are considered as promising heterogeneous catalysts for organic transformations including oxidation reactions.[76, 77] MOFs have previously served as heterogeneous catalysts in the aerobic oxidation of cycloalkanes, hydrocarbons, benzyl alcohol, thiols, amines and sulfides.[78] Recently, research interest in the construction of MOF-type heterogeneous catalysts for the aerobic oxidation of organic substrates is growing rapidly.[76] Inspired by these observations, we have investigated the catalytic activity of **1'** using thiophenol as a model substrate under oxygen atmosphere as shown in Scheme 1.

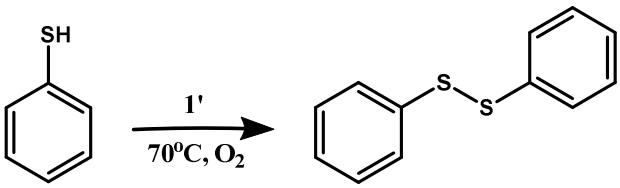

Scheme 1. Oxidation of thiophenol to 1,2-diphenyldisulfide in presence of catalyst **1'** and molecular oxygen.

Aerobic oxidation of thiophenol in the absence of **1'** exhibited only 9% conversion at 70 °C in methanol after 12 h (entry 1, Table 2). In sharp contrast, the oxidation of thiophenol with **1'** using *tert*-butylhydroperoxide (TBHP) as an oxidant resulted in 65% conversion after 12 h in acetonitrile (entry 2, Table 2). On the other hand, the oxidation of thiophenol using molecular oxygen afforded 22% conversion (entry 3, Table 2) in acetonitrile under same conditions. Interestingly, the aerobic oxidation of thiophenol afforded quantitative conversion to

CrystEngComm Accepted Manuscript

Please do not adjust margins

View Article Online
DOI: 10.1039/C7CE01053B

Published on 06 September 2017. Downloaded by Fudan University on 06/09/2017 04:30:45.

the corresponding 1,2-diphenyldisulfide in the presence of **1'** as catalyst in methanol (entry 4, Table 2) after 12 h. The time-conversion curve for the oxidation of thiophenol by employing **1'** (catalyst) and molecular oxygen is shown in Fig. 8. Under similar conditions, the oxidation of thiophenol using catalyst **1'** and molecular oxygen in presence of pyridine significantly reduced the conversion of thiophenol to 27% (entry 5, Table 2). This experiment clearly demonstrates the negative role of pyridine by acting as a catalyst poison through coordination with the Lewis acid sites, thus inhibiting the coordination of thiophenol with cerium ions. It has been already reported that ceric ammonium nitrate (CAN) ion is highly effective in the catalytic oxidation of thiols and thioethers utilizing molecular oxygen.[40] In this context, a control experiment in the presence of CAN was performed and the observed results are given in Table 2. It is clear from these data that the reaction proceeds in the presence of CAN, however, it could not reach completion because of the absence of adequate Ce(IV) ions in the reaction medium (entry 6, Table 2). In contrast, the reaction in the presence of **1'** resulted in complete conversion due to the presence of sufficient amount of Ce(IV) ions as active sites in the framework, thus proving the merit of heterogeneity.

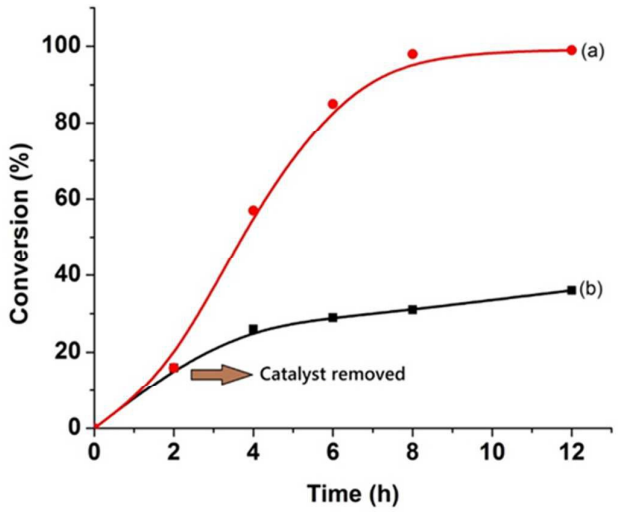

Fig. 8. Hot filtration experiment for the aerobic oxidation of thiophenol (a) with and (b) without **1'**. Reaction conditions: thiophenol (1 mmol), CH_3OH (2 mL), **1'** (20 mg), 70 °C.

Hot filtration experiment was performed in order to verify the heterogeneity of the reaction. Therefore, the oxidation of thiophenol was carried out in presence of **1'** and molecular oxygen under the optimum reaction conditions. The catalyst **1'** was filtered off after 2 h and the reaction was prolonged with the supernatant liquid for another 10 h. The results obtained from these experiments are shown in Fig. 8. These results confirm the heterogeneity of the oxidation catalysis reaction. However, there was marginal enhancement in the conversion of thiophenol after removal of the catalyst, which is indicative of the contribution from blank control. In addition, the recyclability of **1'** for the oxidation of thiophenol with molecular oxygen was examined under the optimized reaction conditions. The conversion of thiophenol observed in the 1st, 2nd, 3rd and 4th cycles after 12 h corresponded to 100%, 98%, 97% and 96%, respectively (Table 2 and Fig. S47, ESI†). Furthermore, the crystallinity of the catalyst recovered after the 4th cycle was very similar with the fresh **1'**, as corroborated by the corresponding XRPD patterns (Fig. S48, ESI†). The structural robustness of the MOF catalyst during the catalytic cycles was confirmed by these experiments.

Table 2. Oxidation of thiophenol to 1,2-diphenyldisulfide in the presence of **1'** under various conditions.[a]

Sl. No.	Catalyst (mg)	Oxidant	Solvent	Conversion (%)
1	---	O_2	CH_3OH	9
2[b]	20	TBHP	CH_3CN	65
3	20	O_2	CH_3CN	22
4	20	O_2	CH_3OH	100
5[c]	20	O_2	CH_3OH	27
6[d]	27	O_2	CH_3OH	68
7	run-1	O_2	CH_3OH	100
8	run-2	O_2	CH_3OH	98
9	run-3	O_2	CH_3OH	97
10	run-4	O_2	CH_3OH	96

[a] Reaction conditions: thiophenol (1 mmol), solvent (2 mL), **1'** (20 mg), 70 °C, 12 h.

[b] with 1 mmol TBHP.

[c] with 1 mmol pyridine.

[d] with CAN.

The encouraging results concerning the aerobic oxidation of thiophenol using **1'** as a catalyst prompted us to explore the versatility of this catalyst with substituted thiophenols. The results of these experiments are summarized in Table 3. Thiophenols with electron donating substituents such as amino, methyl and methoxy at 2-, 4- and 4-positions exhibited respective disulfides in 71, 97 and 59% yields after 12 h (entries 2-4, Table 3). On the other hand, thiophenols containing electron withdrawing groups like fluoro, chloro and bromo at 2, 3- and 4-positions resulted in 87, 91 and 82% yields of the corresponding disulfide (entries 5-7, Table 3). Similarly, cyclohexanethiol gave 26% yield of the corresponding disulfide under identical conditions (entry 8, Table 3).

CrystEngComm Accepted Manuscript

This journal is © The Royal Society of Chemistry 20xx

Please do not adjust margins
View Article Online
DOI: 10.1039/C7CE01053B

Published on 06 September 2017. Downloaded by Fudan University on 06/09/2017 04:30:45.

Table 3. Oxidation of various thiophenols in the presence of **1'** and molecular oxygen.[a]

Sl. No.	Thiol	Disulfide	Yield (%)[b]
1		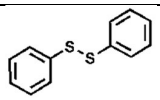	100
2		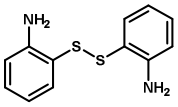	71
3	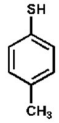	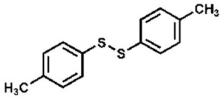	97
4	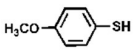	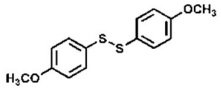	59
5		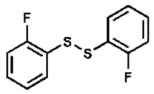	87
6	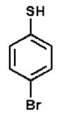	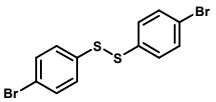	82
7		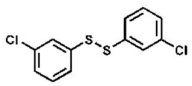	91
8		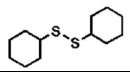	26

[a] Reaction conditions: Thiol (1 mmol), **1'** (20 mg), methanol (2 mL), 70 °C, 12 h, molecular oxygen.

[b] Deduced by GC employing external standard method.

Conclusions

We have successfully synthesized a cerium-based MOF material (**1**) incorporating 3,4-dimethylthieno[2,3-b]thiophene-2,5-dicarboxylic acid as ligand under solvothermal conditions. For ensuring the phase-purity of the material, a comprehensive characterization was carried out by employing methods like XRPD, XPS, FT-IR spectroscopy, TG and N_2 sorption experiments. According to the N_2 sorption experiments, **1'** exhibited a large specific BET surface area (1020 m^2 g^{-1}). As gleaned from the XRPD measurements, the material displayed high structural robustness in water, 1M HCl and acetic acid. Remarkably, the compound showed an intrinsic oxidase-mimic catalytic activity due to the existence of redox-active cerium atoms in the framework. The excellent oxidase-like catalytic properties of the material was demonstrated by employing the typical chromogenic peroxidase substrates: TMB and AzBTS. The oxidase-mimic activity of **1'** allowed us to establish a colorimetric sensing platform for biothiols in NaAc buffer (0.2 M, pH = 4). In addition, the MOF displayed sensing ability towards cysteine in human blood plasma. Owing to the existence of framework Ce(III)/Ce(IV) sites, significant heterogeneous catalytic performance of **1'** was observed in the oxidation of thiol compounds using molecular oxygen. The MOF material is reusable, both as a heterogeneous catalyst as well as a colorimetric biosensor. Moreover, the compound is highly stable, low-cost and recyclable. These features along with high biomimetic and heterogeneous catalytic activities make the present compound suitable for biological sample analysis, medical diagnostics as well as for industrial oxidation catalysis.

Acknowledgements

SB would like to acknowledge financial assistance from Science and Engineering Research Board (SERB; grant no. EEQ/2016/000012), New Delhi. The Central Instruments Facility (CIF) of IIT Guwahati is acknowledged facility for analytical facility. We are thankful to Ministry of Human Resource Development for Center of Excellence in FAST (grant no. F. No. 5-7/2014-TS-VII). We are also thankful to Dr. Chinnakonda S. Gopinath (NCL, Pune, India) for XPS analysis. AD thanks the University Grants Commission (UGC), New Delhi, for the award of an Assistant Professorship under its Faculty Recharge Programme. AD also thanks the Department of Science and Technology, India, for the financial support through Extra Mural Research Funding (EMR/2016/006500).

Notes and references

1. T. R. Lin, L. S. Zhong, L. Q. Guo, F. F. Fu and G. N. Chen, *Nanoscale*, 2014, **6**, 11856-11862.
2. Y. Song, W. Wei and X. Qu, *Adv. Mater.*, 2011, **23**, 4215-4236.
3. M. A. Mansoor, A. M. Svardal and P. M. Ueland, *Anal. Biochem.*, 1992, **200**, 218-229.
4. T. W. Kang, S.-J. Jeon, H.-I. Kim, J. H. Park, D. Yim, H.-R. Lee, J.-M. Ju, M.-J. Kim and J.-H. Kim, *ACS Nano*, 2016, **10**, 5346–5353.
5. H. Cahová, L. Havran, P. Brázdilová, H. Pivoňková, R. Pohl, M. Fojta and M. Hocek, *Angew. Chem.*, 2008, **120**, 2089-2092.
6. Y. Shao, J. Wang, H. Wu, J. Liu, I. A. Aksay and Y. Lin, *Electroanalysis*, 2010, **22**, 1027-1036.
7. V. L. Arcus, E. J. Prentice, J. K. Hobbs, A. J. Mulholland, M. W. Van der Kamp, C. R. Pudney, E. J. Parker and L. A. Schipper, *Biochemistry*, 2016, **55**, 1681-1688.
8. Y. Lin, J. Ren and X. Qu, *Acc. Chem. Res.*, 2014, **47**, 1097-1105.
9. M. Liang, K. Fan, Y. Pan, H. Jiang, F. Wang, D. Yang, D. Lu, J. Feng, J. Zhao and L. Yang, *Anal. Chem.*, 2012, **85**, 308-312.

CrystEngComm Accepted Manuscript

Please do not adjust margins

View Article Online
DOI: 10.1039/C7CE01053B

Published on 06 September 2017. Downloaded by Fudan University on 06/09/2017 04:30:45.

10. J. Liu and Y. Lu, *J. Am. Chem. Soc.*, 2003, **125**, 6642-6643.
11. Y. Zhang, J. Zhang, X. Huang, X. Zhou, H. Wu and S. Guo, *Small*, 2012, **8**, 154-159.
12. H. Li, W. Kong, J. Liu, M. Yang, H. Huang, Y. Liu and Z. Kang, *J. Mater. Chem. B*, 2014, **2**, 5652-5658.
13. S. Song, Y. Qin, Y. He, Q. Huang, C. Fan and H.-Y. Chen, *Chem. Soc. Rev.*, 2010, **39**, 4234-4243.
14. A. Saxena, A. Kumar and S. Mozumdar, *J. Mol. Catal. A: Chem.*, 2007, **269**, 35-40.
15. H. P. Xiang, M. Z. Rong and M. Q. Zhang, *ACS Sustainable Chem. Eng.* , 2016, **4**, 2715-2724.
16. A. Ogawa, Y. Nishiyama, N. Kambe, S. Murai and N. Sonoda, *Tetrahedron Lett.*, 1987, **28**, 271-3274.
17. M. H. Ali and M. McDermott, *Tetrahedron Lett.*, 2005, **46**, 3583-3585.
18. K. Roy and C. S. Gopinath, *Anal. Chem.*, 2014, **86**, 3683-3687
19. K. Roy, C. P. Vinod and C. S. Gopinath, *J. Phys. Chem. C*, 2013, **117**, 4717-4726.
20. Z. Kang, L. Fan and D. Sun, *J. Mater. Chem. A*, 2017, **5**, 10073-10091.
21. J.-W. Zhang, H.-T. Zhang, Z.-Y. Du, X. Wang, S.-H. Yu and H.-L. Jiang, *Chem. Commun.*, 2014, **50**, 1092-1094.
22. D. Chen, B. Li, L. Jiang, D. Duan, Y. Li, J. Wang, J. He and Y. Zeng, *RSC Adv.*, 2015, **5**, 97910-97917.
23. F. Cui, Q. Deng and L. Sun, *RSC Adv.*, 2015, **5**, 98215-98221
24. L. Ai, L. Li, C. Zhang, J. Fu and J. Jiang, *Chem. Eur. J.*, 2013, **19**, 15105-15108.
25. Z. Yuan, F. Lu, M. Peng, C.-W. Wang, Y.-T. Tseng, Y. Du, N. Cai, C.-W. Lien, H.-T. Chang, Y. He and E. S. Yeung, *Anal. Chem.*, 2015, **87**, 7267–7273.
26. Y. L. Liu, X. J. Zhao, X. X. Yang and Y. F. Li, *Analyst*, 2013, **138**, 4526–4531.
27. Z. J. Sun, J. Z. Jiang and Y. F. Li, *Analyst*, 2015, **140**, 8201-8208.
28. Y. Wang, Y. Zhu, A. Binyam, M. Liu, Y. Wu and F. Li, *Biosens. Bioelectron.*, 2016, **86**, 432-.
29. D. Feng, Z.-Y. Gu, J.-R. Li, H.-L. Jiang, Z. Wei and H.-C. Zhou, *Angew. Chem. Int. Ed.*, 2002, **51**, 10307-10310.
30. Y. Chen, T. Hoang and S. Ma, *Inorg. Chem.*, 2012, **51**, 12600-12602.
31. Z. W. Jiang, Y. Liu, X. Hu and Y. Li, *Anal. Methods*, 2014, **6**, 5647-5651.
32. Y. Xiong, S. Chen, F. Ye, L. Su, C. Zhang, S. Shen and S. Zhao, *Chem. Commun.*, 2015, **51**, 4635-4638.
33. Z. Hu, X. Jiang, F. Xu, J. Jia, Z. Long and X. Hou, *Talanta*, 2016, **158**, 276-282.
34. A. Dhakshinamoorthy, M. Alvaro and H. Garcia, *Chem. Commun.*, 2010, **46**, 6476-6478.
35. I. Celardo, J. Z. Pedersen, E. Traversa and L. Ghibelli, *Nanoscale*, 2011, **3**, 1411-1420.
36. A. Asati, S. Santra, C. Kaittanis, S. Nath and J. M. Perez, *Angew. Chem. Int. Ed.*, 2009, **48**, 2308-2312.
37. D. H. Kim, J. Hur, H. G. Park and M. I. Kim, *Biosens. Bioelectron.*, 2017, **93**, 226-233.
38. M. Ornatska, E. Sharpe, D. Andreescu and S. Andreescu, *Anal. Chem.*, 2011, **83**, 4273–4280.
39. H. Firouzabadi, N. Iranpoor, H. Parham, A. Sardarian and J. Toofan, *Synth. Commun.*, 1984, **14**, 717-723.
40. V. Sridharan and J. C. Menéndez, *Chem. Rev.*, 2010, **110**, 3805-3849.
41. S. H. Mashraqui, H. Hariharasubrahmanian and S. Kumar, *Synthesis*, 1999, 2030-2032.
42. S. Mostakim, M. Grzywa, D. Volkmer and S. Biswas, *J. Solid State Chem.*, 2015, **232**, 221-227.
43. K. Wang, H. Huang, W. Xue, D. Liu, X. Zhao, Y. Xiao, Z. Li, Q. Yang, L. Wang and C. Zhong, *CrystEngComm*, 2015, **17**, 3586-3590.
44. L. Valenzano, B. Civalleri, S. Chavan, S. Bordiga, M. H. Nilsen, S. Jakobsen, K. P. Lillerud and C. Lamberti, *Chem. Mater.*, 2011, **23**, 1700-1718.
45. C. Hennig, A. Ikeda-Ohno, W. Kraus, S. Weiss, P. Pattison, H. Emerich, P. M. Abdala and A. C. Scheinost, *Inorg. Chem.*, 2013, **52**, 11734-11743.
46. R. Jain, A. Dubey, M. K. Ghosalya and C. S. Gopinath, *Catal. Sci. Technol.*, 2016, **6**, 1746-1756.
47. E. Bêche, P. Charvin, D. Perarnau, S. Abanades and G. Flamant, *Surf. Interface Anal.*, 2008, **40**, 264-267.
48. G. Zhou, Y. Yao, X. Zhao, X. Liu, B. Sun and A. Zhou, *RSC Adv.*, 2016, **6**, 59370-59374.
49. M. S. P. Francisco, V. R. Mastelaro, P. A. P. Nascente and A. O. Florentino, *J. Phys. Chem. B*, 2001, **105**, 10515-10522.
50. S. Garain, K. Barman, T. K. Sinha, S. Jasimuddin, J. Haeberle, K. Henkel, D. Schmeisser and D. Mandal, *ACS Appl. Mater. Interfaces*, 2016, **8**, 21294−21301.
51. R. Dalapati and S. Biswas, *Sens. Actuators., B*, 2017, **239**, 759-767.
52. R. Dalapati, B. Sakthivel, A. Dhakshinamoorthy, A. Buragohain, A. Bhunia, C. Janiak and S. Biswas, *CrystEngComm*, 2016, **18**, 7855-7864.
53. F.-X. Qin, S.-Y. Jia, F.-F. Wang, S.-H. Wu, J. Song and Y. Liu, *Catal. Sci. Tech.*, 2013, **3**, 2761-2768.
54. Y. Chen, V. Lykourinou, T. Hoang, L.-J. Ming and S. Ma, *Inorg. Chem*, 2012, **51**, 9156-9158.
55. H. Tan, Q. Li, Z. Zhou, C. Ma, Y. Song, F. Xu and L. Wang, *Anal. Chim. Acta*, 2015, **856**, 90–95.
56. Y. L. Liu, W. L. Fu, C. M. Li, C. Z. Huang and Y. F. Li, *Anal. Chim. Acta*, 2015, **861**, 55-61.
57. Q. Zhu, Y. Chen, W. Wang, H. Zhang, C. Ren, H. Chen and X. Chen, *Sens. Actuators, B.*, 2015, **210**, 500-507.
58. F. Luo, Y. Lin, L. Zheng, X. Lin and Y. Chi, *ACS Appl. Mater. Interfaces*, 2015, **7**, 11322-11329.
59. J.-W. Zhang, H.-T. Zhang, Z.-Y. Du, X. Wang, S.-H. Yu and H.-L. Jiang, *Chem. Commun.*, 2014, **50**, 1092-1094.
60. D. Chen, B. Li, L. Jiang, D. Duan, Y. Li, J. Wang, J. He and Y. Zeng, *RSC Adv.*, 2015, **5**, 97910-97917.
61. L. Su, Y. Xiong, H. Yang, P. Zhang and F. Ye, *J. Mater. Chem. B*, 2016, **4**, 128-134.
62. Y. Chen, V. Lykourinou, T. Hoang, L.-J. Ming and S. Ma, *Inorg. Chem.*, 2012, **51**, 9156−9158.

CrystEngComm Accepted Manuscript

This journal is © The Royal Society of Chemistry 20xx

Please do not adjust margins
View Article Online
DOI: 10.1039/C7CE01053B

63. Y. Chen, T. Hoang and S. Ma, *Inorg. Chem.*, 2012, **51**, 12600−12602.
64. D. Feng, Z.-Y. Gu, J.-R. Li, H.-L. Jiang, Z. Wei and H.-C. Zhou, *Angew. Chem. Int. Ed.*, 2012, **51**, 10307–10310
65. Y. Chen and S. Ma, *Dalton Trans.*, 2016, **45**, 9744-9753.
66. K. Müller-Buschbaum, F. Beuerle and C. Feldmann, *Microporous Mesoporous Mater.*, 2015, **216**, 171-199.
67. E.-L. Zhou, C. Qin, P. Huang, X.-L. Wang, W.-C. Chen, K.-Z. Shao and Z.-M. Su, *Chem. Eur. J.*, 2015, **21**, 11894-11898.
68. X. Zhang, X. Bi, W. Di and W. Qin, *Sens. Actuators, B.*, 2016, **231**, 714-722.
69. A. Garcia-Leis, D. Jancura, M. Antalik, J. Garcia-Ramos, S. Sanchez-Cortes and Z. Jurasekova, *Phys. Chem. Chem. Phys.*, 2016, **18**, 26562-26571.
70. Z. Hu, X. Jiang, F. Xu, J. Jia, Z. Long and X. Hou, *Talanta*, 2016, **158**, 276-282.
71. H. S. Jung, X. Chen, J. S. Kim and J. Yoon, *Chem. Soc. Rev.*, 2013, **42**, 6019-6031.
72. Y. Xiong, S. Chen, F. Ye, L. Su, C. Zhang, S. Shen and S. Zhao, *Chem. Commun.*, 2015, **51**, 4635-4638.
73. Y. Liu, X. Lv, M. Hou, Y. Shi and W. Guo, *Anal. Chem.*, 2015, **87**, 11475–11483.
74. R. S. Vasan, A. Beiser, R. B. D'Agostino, D. Levy, J. Selhub, P. F. Jacques, I. H. Rosenberg and P. W. F. Wilson, *JAMA*, 2003, **289(10)**, 1251-1257.
75. D. Ścibior, M. Skrzycki, M. Podsiad and H. Czeczot, *Clin. Biochem.*, 2008, **41**, 852–858.
76. A. Dhakshinamoorthy, A. M. Asiri and H. Garcia, *Chem. Eur. J.*, 2016, **22**, 8012-8024.
77. A. Dhakshinamoorthy, M. Alvaro and H. Garcia, *Catal. Sci. Technol.*, 2011, **1**, 856-867.
78. A. Dhakshinamoorthy, M. Alvaro and H. Garcia, *Chem. Commun.*, 2012, **48**, 11275-11288.

Table of Contents:

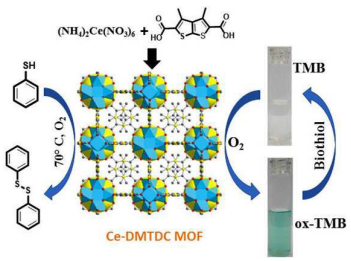

A cerium-based MOF has been reported to exhibit oxidase-mimic activity for colorimetric sensing of biothiols and aerobic oxidation of thiols.

Published on 06 September 2017. Downloaded by Fudan University on 06/09/2017 04:30:45.
CrystEngComm Accepted Manuscript

Please do not adjust margins